

LBP-Motivated Colour Texture Classification

Raquel Bello-Cerezo^{1,*}, Paul Fieguth², and Francesco Bianconi¹

¹ Department of Engineering, Università degli Studi di Perugia
Via Goffredo Duranti 93, 06125 Perugia, Italy
{bellocerezo@gmail.com, bianco@ieee.org}

² Systems Design Engineering, University of Waterloo
200 University Avenue West, N2L 3G1 Waterloo, ON, Canada
pfieguth@uwaterloo.ca

Abstract. In this paper we investigate extensions of Local Binary Patterns (LBP), Improved Local Binary Patterns (ILBP) and Extended Local Binary Patterns (ELBP) to colour textures via two different strategies: intra-/inter-channel features and colour orderings. We experimentally evaluate the proposed methods over 15 datasets of general and biomedical colour textures. Intra- and inter-channel features from the RGB space emerged as the best descriptors and we found that the best accuracy was achieved by combining multi-resolution intra-channel features with single-resolution inter-channel features.

Keywords: Colour, Texture, Local Binary Patterns

1 Introduction

Colour and texture, along with transparency and gloss, are among the most important visual features of objects, materials and scenes. As a consequence, colour and texture analysis plays a fundamental role in many computer vision applications such as surface inspection [1–3], medical image analysis [4–7] and object recognition [8–10]. It is generally believed that combining colour and texture improves accuracy (at least under steady imaging conditions [11, 12]), though it is not quite clear which is the best way to do it. Indeed this has been subject of debate since early on, both in computer vision [11, 12] and perception science [13].

Approaches to colour texture analysis can be roughly categorised into three groups: *parallel*, *sequential* and *integrative* [14], though more involved taxonomies have been proposed too [15]. In this paper we investigate the problem of representing colour texture features starting from three LBP variants as grey-scale texture descriptors. Even in the era of Deep Learning, there are good reasons why Local Binary Patterns and related variations are worth investigating: they

*Performed part of this work as a visiting graduate student in the Systems Design Engineering department at the University of Waterloo, Canada.

are conceptually simple, compact, easy to implement, computationally cheap – yet very accurate. We consider two strategies to extend LBP variants to colour textures: the combination of inter- and intra-channel features, and colour orderings. We also evaluate the effect of the colour space used (RGB, HSV, YUV and YIQ) and of the spatial resolution(s) of the local neighbourhood.

2 Background: Grey-Scale LBP Variants

Local Binary Patterns variants [16–22] (also referred to as *Histograms of Equivalent Patterns* [23]) are a well-known class of grey-scale texture descriptors. They are particularly appreciated for their conceptual ease, low computational demand yet high discrimination capability. Nonetheless, extensions to colour images have received much less attention than the original, grey-scale descriptors. In this paper we investigate extensions to the colour domain of Local Binary Patterns [16], Improved Local Binary Patterns [24] and Extended Local Binary Patterns [25], though the same methods could be easily extended to other descriptors of the same class (see [22] for an up-to-date review).

The three methods are all based on comparing the grey-levels of the pixels in a neighbourhood of given shape and size, but the comparison scheme is different in the three cases (see [16, 24, 25] for details). In general, any such comparison scheme can be regarded as a hand-designed function (also referred to as the *kernel function* [23]), which maps a local image pattern to one visual word among a set of pre-defined ones (dictionary). In formulas, denoted with \mathcal{N} the neighbourhood, \mathcal{P} a local image pattern (set of grey-scale values over that neighbourhood) and f the kernel function we can write:

$$\mathcal{P} \xrightarrow{f} w; \quad w \in \{w_1, \dots, w_K\}, \quad (1)$$

where $\{w_1, \dots, w_K\}$ is the dictionary. Consequently, any LBP variant identifies with its kernel function and vice-versa, as clearly shown in [26]. The dimension of the dictionary depends on the kernel function and the number of pixels in the neighbourhood: standard LBP [16, 18, 19] for instance generates a dictionary of 2^{n-1} words, being n the number of pixels in the neighbourhood. Image features are the one-dimensional, orderless distribution of the visual words over the dictionary (bag of visual words model).

Rotation-invariant versions of LBP and variants are computed by grouping together the visual words that can be obtained from one another via a discrete rotation of the peripheral pixels (also usually referred to as the ‘*ri*’ configuration [16]). In this case the dimension of the (reduced) dictionary can be computed through standard combinatorial methods [27].

3 Extensions to Colour Images

3.1 Intra- and Inter-channel Analysis

Intra- and/or inter-channel analysis are classic tools for extending texture descriptors to colour images [28–30]. Intra-channel features are computed from

each colour channel separately, inter-channel features from pairs of channels. In both cases the resulting features are concatenated into a single vector. As for inter-channel features, if we consider three-channel images and indicate with i , j and k the colour channels, there are six possible combinations: ij , ik , jk , ji , ki and kj . However, to avoid redundancy and reduce the overall number of features, it is customary to retain only the first three [29, 30]. Figures 1 and 2 show how to compute intra- and inter-channel features in the RGB space.

Intra- and inter-channel analysis applies to grey-scale LBP variants by replacing the comparison between the grey levels with that between the intensity levels within each colour channel and/or pairs of them, respectively. Therefore, both intra- and inter-channel analysis multiply by three the dimension of the original descriptor (by six when used together). Intra- and inter-channel analysis extends LBP, ILBP and ELBP seamlessly to the colour domain. In the remainder we refer to these colour extensions respectively as Opponent Colour LBP (OCLBP) [29], Improved Opponent Colour LBP (IOCLBP) [30] and Extended Opponent Colour LBP (EOCLBP).

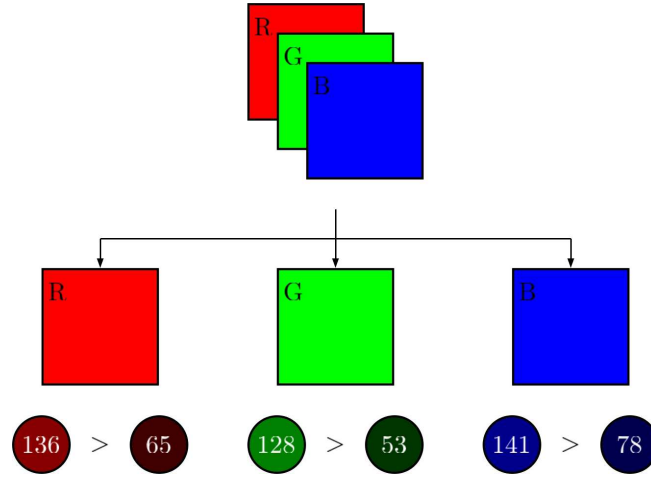


Fig. 1. Computing intra-channel features in the RGB space: the intensity values (circles in the figure) are compared within each of the R, G and B channels separately (squares in the figure)

3.2 Colour Orderings

Differently from grey-scale, colour data are multivariate, hence lack a natural ordering. Still, higher-dimension analogues of univariate orderings can be introduced by recurring to some *sub-* (i.e. less than total) *ordering* principles [31]. Herein we considered the following three types of sub-orderings in the colour

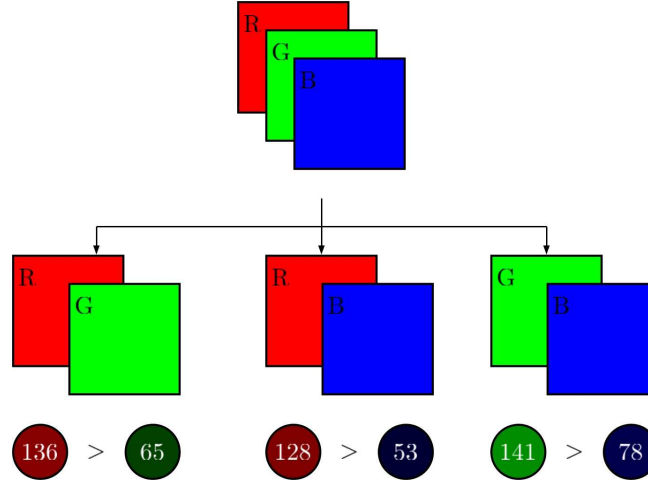


Fig. 2. Computing inter-channel features in the RGB space: the intensity values (circles in the figure) are compared between each of the R/G, R/B and G/B pairs of colour channels (squares in the figure)

space: *lexicographic order*, *order based on the colour vector norm* and *order based on a reference colour* [32–37]. The first is a marginal ordering (M-ordering), the second and third are reduced (or aggregate) orderings (R-orderings) [31]. In the remainder we use subscripts ‘lex’, ‘cvn’ and ‘rel’ to indicate the three orderings. Once the order is defined, the grey-scale descriptors introduced in Section 2 extend seamlessly to the colour domain. Also note that colour orderings produce more compact descriptors than intra- and inter-channel analysis, for the number of features is, in this case, the same as that of the original grey-scale descriptor.

Lexicographic Order The lexicographic order [32, 34] involves defining some kind of (arbitrary) priority among the colour channels. Denoted with i , j and k the three channels, one can for instance establish that i has higher priority than j and j higher than k . In that case, given two colours $\mathbf{C}_1 = \{C_{1i}, C_{1j}, C_{1k}\}$ and $\mathbf{C}_2 = \{C_{2i}, C_{2j}, C_{2k}\}$, we shall write:

$$\mathbf{C}_1 \geq \mathbf{C}_2 \iff (C_{1i} > C_{2i}) \vee [(C_{1i} = C_{2i}) \wedge (C_{1j} > C_{2j})] \vee [(C_{1i} = C_{2i}) \wedge (C_{1j} = C_{2j}) \wedge (C_{1k} \geq C_{2k})]. \quad (2)$$

For three-dimensional colour data there are $3! = 6$ priority rules, and, consequently, as many lexicographic orders.

Aggregate Order Based on the Colour Vector Norm This is based on comparing the vector norm [33] of the two colours:

$$\mathbf{C}_1 \geq \mathbf{C}_2 \iff \|\mathbf{C}_1\| \geq \|\mathbf{C}_2\|, \quad (3)$$

where ‘ $\|\cdot\|$ ’ indicates the vector norm. In the remainder we shall assume that this be the L_2 norm, although other types of distance can be used as well.

Aggregate Order Based on a Reference Colour In this case the comparison is based on the distance from a given (and again arbitrary) reference colour \mathbf{C}_{ref} [35]:

$$\mathbf{C}_1 \geq \mathbf{C}_2 \iff \|\mathbf{C}_1 - \mathbf{C}_{\text{ref}}\| \geq \|\mathbf{C}_2 - \mathbf{C}_{\text{ref}}\|. \quad (4)$$

Clearly this case reduces to the order based on the colour vector norm when $\mathbf{C}_{\text{ref}} = \{0, 0, 0\}$.

4 Experiments

Different strategies have been proposed to extend LBP (and variants) to colour textures. In order to evaluate the effectiveness of the approaches described in Section 3 and to explore which one works better in the case of colour images, we carried out a set of supervised image classification experiments using 15 colour texture datasets (more details on this in Section 5). We first run a group of three experiments to determine the optimal settings regarding the colour space used (Experiment 1), the colour orderings (Experiment 2) and the combination of resolutions for intra- and inter-channel features (Experiment 3). To reduce the overall computational burden we only used datasets #1 to #5 for this first group of experiments. Finally, in the last experiment we selected the best settings and carried out a comprehensive evaluation using all the datasets.

We computed rotation-invariant (‘*ri*’) features from non-interpolated pixel neighbourhoods of radius 1px, 2px and 3px (Fig. 3) and concatenated them. In the remainder, symbol ‘&’ will indicate concatenation; therefore we shall write, for instance, ‘1&2&3’ to signal concatenation of the feature vectors computed at resolution 1, 2 and 3.

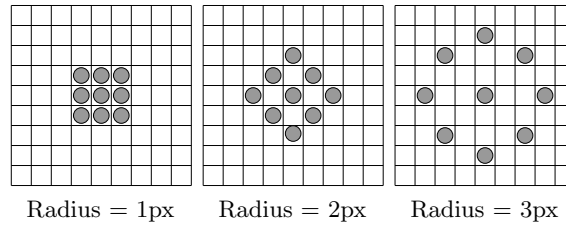


Fig. 3. Pixel neighbourhoods corresponding to resolutions 1, 2 and 3, respectively

The accuracy was estimated via split sample validation with stratified sampling using a train ratio of 1/2, i.e.: half of the samples of each class (train set) were used to train the classifier and the remaining half (test set) to compute the figure of merit. This was the fraction of samples of the test set classified correctly. Classification was based on the nearest neighbour rule with L_1 ('city-block') distance.

4.1 Experiment 1: Selecting the Best Colour Space for Intra- and Inter-channel Features

This experiment aimed to determine the best colour space among RGB, HSV, YUV and YIQ (conversion formulae from RGB available in [38]). Since HSV separates colour into heterogeneous components (hue, saturation and value), we also used a normalized version of this space (HSV_{norm} in the remainder):


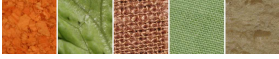
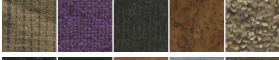
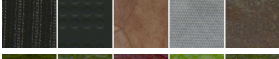
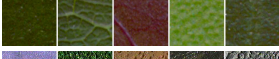

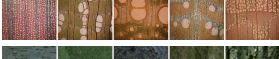

$$\begin{aligned} H_{\text{norm}} &= \frac{H - \mu_H}{\sigma_H}, \\ S_{\text{norm}} &= \frac{S - \mu_S}{\sigma_S}, \\ V_{\text{norm}} &= \frac{V - \mu_V}{\sigma_V}. \end{aligned} \tag{5}$$

where μ and σ indicate the average values over the input image. Normalized versions of YUV and YIQ were also considered, but not reported in the results owing to their poor performance. We computed both intra- and inter-channel features at resolutions 1, 2 and 3, and concatenated the results ('1&2&3'). We considered the following combinations of colour spaces respectively for the intra- and inter-channel features: RGB-RGB, HSV-HSV, HSV-RGB, HSV- HSV_{norm} , HSV-YUV and HSV-YIQ (see Table 3, boldface figures).

4.2 Experiment 2: Colour Orderings Vs. Intra- and Inter-channel Features

The objective of this experiment was to evaluate the effectiveness of intra- and inter-channel features compared with colour orderings (Section 3.2) in the RGB colour space, which emerged as the best one from Experiment 1. For the lexicographic order we considered all the six possible combinations of priority among the R, G and B channels, though for the sake of simplicity we only report (see Table 4) the results of the combination that attained the best accuracy in the majority of the cases (this was $G \succ R \succ B$). For the order based on a reference colour we considered three possible references, the same three used in [36] since they were the best among the eight vertices of the RGB colour cube: white (1,1,1), green (0,1,0) and magenta (1,0,1), and the first gave the best results (see Table 4). As in Experiment 1, the image features were computed at resolution 1, 2 and 3 and the resulting vectors concatenated ('1&2&3').

Table 1. Summary table of the generic colour texture datasets used in the experiments

ID	Name	No. of classes	No. of samples per class	Size (px×px)	Sample images
1	KTH-TIPS	10	81	200×200	
2	KTH-TIPS2b	11	432	200×200	
3	Outex-00013	68	20	128×128	
4	Outex-00014	68	60	128×128	
5	PlantLeaves	20	60	128×128	
6	CUReT	61	92	128×128	
7	ForestSpecies	112	20	768×768	
8	NewBarkTex	6	272	64×64	

4.3 Experiment 3: Selecting Optimal Resolutions for Intra- and Inter-channel Features

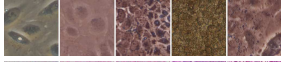
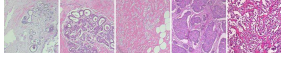
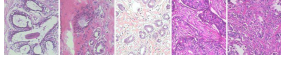
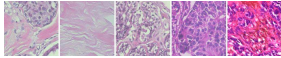
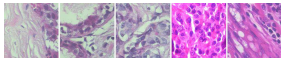
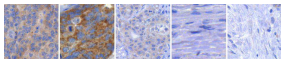
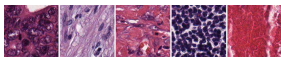
Since the use of intra- and inter-channel analysis increased by six the number of features of grey-scale descriptors, in this experiment we investigated how to reduce the overall number of features – this way generating reasonably compact descriptors – by selecting appropriate resolutions for intra- and inter-channel features. Specifically, we used three concatenated resolutions (‘1&2&3’) for intra-channel features and one (‘1’, ‘2’ or ‘3’) or two concatenated resolutions (‘1&2’, ‘1&3’ or ‘2&3’) for inter-channel features.

4.4 Experiment 4: Overall Evaluation with Optimised Settings

In this last experiment we computed the classification accuracy over all the 15 datasets described in Section 5 using the settings that emerged as optimal from the previous experiments. For calibration purposes we also included five pre-trained convolutional neural network models – specifically: three residual networks (ResNet-50, ResNet-101 and ResNet-152 [39]) and two VGG ‘very deep’ models (VGG-VeryDeep-16 and VGG-VeryDeep-19 [40]). Image features in this case were the L_1 normalised output of the last fully-connected layer (usually referred to as the ‘FC’ configuration [41, 42]). The results are reported in Tables 6– 7.

Table 3 summarises the results of Experiment 1. As can be seen, the RGB-RGB combination for intra- and inter-channel features emerged as the best op-

Table 2. Summary table of the biomedical textures used in the experiments

ID	Name	No. of classes	No. of samples per class	Size (px×px)	Sample images
9	BioMediTechRPE	4	150–949	480×480	
10	BreakHis 40×	2	625–1370	460×460	
11	BreakHis 100×	2	644–1437	460×460	
12	BreakHis 200×	2	623–1390	460×460	
13	BreakHis 400×	2	588–1232	460×460	
14	Epistroma	2	551–825	Variable	
15	Kather	8	625	150×150	

tion in seven datasets, followed by HSV-HSV (five datasets) and HSV-RGB (four datasets).

5 Datasets

For the experimental evaluation we considered eight datasets of generic colour textures and seven of biomedical textures as detailed in Sections 5.1– 5.2. The main characteristics of each dataset are also summarised in Tables 1– 2.

5.1 Generic Colour Textures

#1 – #2: KTH-TIPS [43, 44] and KTH-TIPS2b [45, 44]. Generic materials as *bread, cotton, cracker, linen, orange peel, sandpaper, sponge* or *styrofoam*, acquired at nine scales, three viewpoints and three different illuminants.

#3 – #4: Outex-00013 [16, 46] and Outex-00014 [16, 46]. Generic materials such as *carpet, chips, flakes, granite, paper, pasta* or *wallpaper*. Images from Outex-00013 were acquired under invariable imaging conditions and those from Outex-00014 under three different illumination conditions.

#5, #7 – #8: PlantLeaves [47], ForestSpecies [48, 49] and NewBarkTex [50, 51]. Images from different species of plants, trees and bark acquired under controlled and steady imaging conditions.

#6: CURET [52]. A reduced version of the Columbia-Utrecht Reflectance and Texture database maintained by the Visual Geometry Group, University of Oxford, United Kingdom [53], containing samples of generic materials.

Table 3. Results of Experiment 1: selecting the best colour space for intra- and inter-channel features. Boldface text indicates the best combination descriptor + colour spaces; framed text the overall best accuracy by dataset. Although the KTH-TIPS and KTH-TIPS2b datasets saw improvements with HSV, all other datasets performed best by remaining in RGB space. Classifier was 1-NN (L_1)

Descriptor-[1&2&3]	Colour space	Datasets				
	Intra-Inter	#1	#2	#3	#4	#5
OCLBP	RGB-RGB	95.2	97.8	90.9	91.5	76.9
OCLBP	HSV-HSV	96.6	97.5	91.9	86.7	71.0
OCLBP	HSV-RGB	96.0	98.4	90.4	90.3	73.7
OCLBP	HSV-HSV _{norm}	96.0	97.8	84.9	84.5	73.8
OCLBP	HSV-YUV	92.5	96.2	86.5	84.8	72.6
OCLBP	HSV-YIQ	92.4	96.3	86.6	85.5	74.0
IOCLBP	RGB-RGB	96.2	98.5	91.0	91.9	77.7
IOCLBP	HSV-HSV	97.4	98.2	91.5	87.4	71.9
IOCLBP	HSV-RGB	96.6	98.7	89.4	89.8	73.2
IOCLBP	HSV-HSV _{norm}	96.4	98.1	84.5	85.2	74.0
IOCLBP	HSV-YUV	94.2	97.5	87.9	85.9	73.0
IOCLBP	HSV-YIQ	94.2	97.4	87.8	86.8	74.8
EOCLBP	RGB-RGB	95.3	98.2	91.5	92.0	77.0
EOCLBP	HSV-HSV	97.2	98.5	90.9	87.0	70.7
EOCLBP	HSV-RGB	97.2	98.7	90.4	89.2	70.6
EOCLBP	HSV-HSV _{norm}	96.9	98.2	85.6	85.0	71.7
EOCLBP	HSV-YUV	96.4	98.1	87.3	85.6	71.0
EOCLBP	HSV-YIQ	96.0	98.0	87.2	85.9	71.7
<i>Baseline</i>						
LBP	GREY	94.2	93.5	80.9	83.7	73.8
ILBP	GREY	95.4	95.1	85.5	88.6	76.9
ELBP	GREY	94.5	94.5	84.6	87.4	78.3

5.2 Biomedical Textures

The following databases were acquired through digital microscopy under fixed and reproducible conditions, and are therefore intrinsically different from those presented in the preceding section.

#9: BioMediTechRPE [54, 55]. Retinal pigment epithelium (RPE) cells from different stages of maturation.

#10 – #13: BreakHis [56, 57]. Histological images from benign/malignant breast cancer tissue. Each image was taken under four magnification factors ($40\times$, $100\times$, $200\times$ and $400\times$), and we considered each factor as making up a different dataset (see Tab. 2).

#14 – #15: Epistroma [58, 5] and Kather [59–61]. Histological images from colorectal cancer tissue representing different tissue sub-types.

Table 4. Results of Experiment 2: colour orderings vs. intra- and inter-channel features. Boldface text indicates, for each dataset, the best accuracy by descriptor + colour ordering; framed text the overall best accuracy by dataset. Colour priority for lexicographic order (‘lex’) was $G \succ R \succ B$, distance for colour vector norm (‘cvn’) was L_2 and reference colour for ‘rcl’ was white (1,1,1). The features were computed on the RGB space. The significant reduction in dimensionality offered by the colour orderings does not lead to any improvement

Descriptor-[1&2&3]	Datasets					No. of features
	#1	#2	#3	#4	#5	
LBP _{lex}	94.3	92.3	79.8	82.9	65.2	108
LBP _{cvn}	94.3	92.3	78.5	81.3	69.9	108
LBP _{rcl}	94.0	92.1	78.6	80.2	71.9	108
ILBP _{lex}	95.0	95.7	84.6	87.8	67.6	213
ILBP _{cvn}	94.9	95.5	83.6	87.5	70.3	213
ILBP _{rcl}	94.7	95.3	83.9	88.2	73.4	213
ELBP _{lex}	94.3	94.2	84.5	86.1	66.7	215
ELBP _{cvn}	94.7	94.1	85.6	86.3	73.7	215
ELBP _{rcl}	94.6	93.8	84.6	86.0	77.3	215
<i>Baseline</i>						
LBP	94.2	93.5	80.9	83.7	73.8	108
ILBP	95.4	95.1	85.5	88.6	76.9	213
ELBP	94.5	94.5	84.6	87.4	78.3	215
OCLBP	95.2	97.8	90.9	91.5	76.9	648
IOCLBP	96.2	98.5	91.0	91.9	77.7	1287
EOCLBP	95.3	98.2	91.5	92.0	77.0	1299

6 Results and Discussion

The results of Experiment 2 (Table 4) show that in most cases intra- and inter-channel features from the RGB space improved the accuracy of the original, grey-scale descriptors by a good margin. By contrast, no clear advantage emerged from using colour orderings as an alternative to grey-scale values.

Experiment 3 indicated that the best accuracy was achieved by concatenating multi-resolution intra-channel features and single-resolution inter-channel features. In fact, adding more than one inter-channel resolution degraded the performance in the majority of cases, as clearly shown in Table 5. The results were however inconclusive as to which resolution (‘1’, ‘2’ or ‘3’) should be used.

The comparison between LBP variants and pre-trained convolutional networks (Experiment 4, Tables 6 and 7) showed nearly perfectly split results, with the former achieving the best performance in seven datasets out of 15 and the reverse occurring in the other eight. Convolutional models seemed better at classifying textures with higher intra-class variability (as a consequence of texture non-stationariness and/or changes in the imaging conditions), as for instance in datasets #1, #2 and #7 (see Section 5.1). Conversely, homogeneous textures acquired under steady imaging conditions (most of the biomedical datasets) were still better classified by LBP variants. This finding generally agrees with those

Table 5. Experiment 3: best combination of resolutions for intra- and inter-channel features. Boldface text indicates, for each dataset, the best combination descriptor + resolutions used for computing the inter-channel features; framed text the overall accuracy by dataset. The features were computed on the RGB space. In general, strongest performance is realized by limiting the number of resolutions associated with inter-channel features. That is, the added information present in multiple inter-channels is more than offset by the decrease in classification performance due to the increase in feature dimensionality

Descriptor-[1&2&3] _{intra}	Datasets					No. of features
	#1	#2	#3	#4	#5	
OCLBP-[1] _{inter}	96.6	98.3	91.3	91.6	78.2	432
OCLBP-[2] _{inter}	96.2	98.1	91.7	92.1	78.6	432
OCLBP-[3] _{inter}	95.9	98.1	91.9	92.5	78.8	432
OCLBP-[1&2] _{inter}	96.1	98.1	91.3	91.7	77.2	540
OCLBP-[1&3] _{inter}	96.0	98.1	91.6	92.3	77.4	540
OCLBP-[2&3] _{inter}	95.8	98.0	91.7	92.4	77.2	540
IOCLBP-[1] _{inter}	97.1	98.7	92.2	92.5	80.2	855
IOCLBP-[2] _{inter}	97.1	98.7	92.3	92.6	79.7	855
IOCLBP-[3] _{inter}	96.8	98.6	92.9	93.0	79.4	855
IOCLBP-[1&2] _{inter}	96.8	98.6	91.4	92.0	78.7	1071
IOCLBP-[1&3] _{inter}	96.6	98.6	91.9	92.3	78.6	1071
IOCLBP-[2&3] _{inter}	96.4	98.5	91.7	92.2	78.5	1071
EOCLBP-[1] _{inter}	96.8	98.4	91.7	91.4	79.5	759
EOCLBP-[2] _{inter}	96.7	98.4	91.8	91.5	79.5	759
EOCLBP-[3] _{inter}	96.6	98.4	91.9	91.5	79.4	759
EOCLBP-[1&2] _{inter}	96.5	98.5	91.7	91.3	78.8	867
EOCLBP-[1&3] _{inter}	96.5	98.5	91.8	91.4	78.8	867
EOCLBP-[2&3] _{inter}	96.5	98.5	91.9	91.5	78.8	867
<i>Baseline</i>						
LBP	94.2	93.5	80.9	83.7	73.8	108
ILBP	95.4	95.1	85.5	88.6	76.9	213
ELBP	94.5	94.5	84.6	87.4	78.3	215
OCLBP	95.2	97.8	90.9	91.5	76.9	648
IOCLBP	96.2	98.5	91.0	91.9	77.7	1287
EOCLBP	95.3	98.2	91.5	92.0	77.0	1299

obtained in previous studies [62]. Pre-trained convolutional networks, however, achieved this result by employing at least twice as many features than LBP variants.

7 Conclusions

In this work we have investigated two strategies for extending LBP variants to the colour domain: intra- and inter-channel features on the one hand and colour orderings on the other. Colour orderings did not prove particularly effective; however, intra- and inter-channel features improved the accuracy of the original, grey-scale descriptors in virtually all the cases. The best results were obtained by combining multi-resolution intra-channel features with single-resolution inter-channel features, and this represents a novel finding. In future works we plan

Table 6. Results of Experiment 4: overall evaluation with optimised settings (datasets #1 to #8). Boldface text indicates, for each dataset, the best combination descriptor + resolutions used for computing the inter-channel features; framed text the overall best accuracy by dataset

Descriptor- [1&2&3] _{intra}	Generic textures								No. of features
	1	2	3	4	5	6	7	8	
OCLBP-[1] _{inter}	96.6	98.3	91.3	91.6	78.2	97.5	76.0	82.9	432
OCLBP-[2] _{inter}	96.2	98.1	91.7	92.1	78.6	97.5	76.1	82.7	432
OCLBP-[3] _{inter}	95.9	98.1	91.9	92.5	78.8	97.7	76.4	83.0	432
IOCLBP-[1] _{inter}	97.1	98.7	92.2	92.5	80.2	98.2	81.9	84.5	855
IOCLBP-[2] _{inter}	97.1	98.7	92.3	92.6	79.7	98.0	82.1	83.8	855
IOCLBP-[3] _{inter}	96.8	98.6	92.9	93.0	79.4	98.1	82.1	83.2	855
EOCLBP-[1] _{inter}	96.8	98.4	91.7	91.4	79.5	98.1	83.0	84.8	759
EOCLBP-[2] _{inter}	96.7	98.4	91.8	91.5	79.5	98.1	83.1	84.8	759
EOCLBP-[3] _{inter}	96.6	98.4	91.9	91.5	79.4	98.0	83.1	84.4	759
<i>Baseline</i>									
OCLBP	95.2	97.8	90.9	91.5	76.9	97.4	74.8	79.9	648
IOCLBP	96.2	98.5	91.0	91.9	77.7	97.7	79.9	80.2	1287
EOCLBP	95.3	98.2	91.5	92.0	77.0	97.6	77.3	79.1	1299
<i>CNNs</i>									
VGG-VD-16-FC	99.4	99.5	84.3	83.5	77.4	97.0	85.6	79.1	4096
VGG-VD-19-FC	99.4	99.4	83.8	82.8	78.0	96.9	82.8	81.6	4096
ResNet-50-FC	99.6	99.7	87.2	86.0	86.6	98.5	93.0	90.7	2048
ResNet-101-FC	99.9	99.7	86.4	85.5	82.1	98.6	92.8	90.5	2048
ResNet-152-FC	99.8	99.8	84.8	84.7	83.9	98.5	91.8	90.9	2048

expand the study to consider more LBP variants [22] and different strategies for compacting the feature vectors [63].

Acknowledgments

R. Bello-Cerezo wants to thank the colleagues at Systems Design Engineering, University of Waterloo, Canada, for the assistance received during her research visit from Sep. 2017 to Feb. 2018. F. Bianconi wishes to acknowledge support from the Italian Ministry of University and Research (MIUR) under the Individual Funding Scheme for Fundamental Research (‘FFABR’ 2017) and from the Department of Engineering at the Università degli Studi di Perugia, Italy, under the Fundamental Research Grants Scheme 2018.

References

1. Weszka, J.S., Rosenfeld, A.: An application of texture analysis to materials inspection. *Pattern Recognition* **8**(4) (1976) 195–200
2. Tsai, D.M., Huang, T.: Automated surface inspection for statistical textures. *Image and Vision Computing* **21**(4) (2003) 307–323

Table 7. Results of Experiment 4: overall evaluation with optimised settings (datasets #9 to #15). Boldface text indicates, for each dataset, the best combination descriptor + resolutions used for computing the inter-channel features; framed text the overall best accuracy by dataset

Descriptor- [1&2&3] _{intra}	Biomedical textures							No. of features
	9	10	11	12	13	14	15	
OCLBP-[1] _{inter}	85.4	92.6	91.8	92.2	91.1	92.3	91.5	432
OCLBP-[2] _{inter}	85.4	92.5	91.6	92.4	91.4	92.5	91.6	432
OCLBP-[3] _{inter}	85.3	92.4	91.3	92.3	91.5	92.6	92.0	432
IOCLBP-[1] _{inter}	85.5	93.6	92.9	93.2	91.7	92.0	92.9	855
IOCLBP-[2] _{inter}	85.4	93.7	92.8	93.3	91.8	92.2	93.1	855
IOCLBP-[3] _{inter}	85.4	94.0	93.0	93.4	92.1	92.8	93.1	855
EOCLBP-[1] _{inter}	85.9	93.7	93.2	93.2	90.7	96.0	93.2	759
EOCLBP-[2] _{inter}	86.0	93.7	93.3	93.3	90.8	96.1	93.2	759
EOCLBP-[3] _{inter}	86.0	93.7	93.1	93.4	90.9	96.1	93.3	759
<i>Baseline</i>								
OCLBP	85.2	91.5	91.2	92.1	90.5	91.8	91.0	648
IOCLBP	85.4	93.1	92.2	92.7	91.0	91.8	92.2	1287
EOCLBP	85.8	92.5	91.6	92.4	90.6	93.1	91.6	1299
<i>CNNs</i>								
VGG-VD-16-FC	86.3	89.7	87.0	87.0	83.4	95.3	86.0	4096
VGG-VD-19-FC	86.5	88.8	86.4	85.6	83.4	94.5	84.1	4096
ResNet-50-FC	87.5	93.4	90.9	91.6	89.8	97.3	89.6	2048
ResNet-101-FC	87.7	93.5	90.6	91.0	88.8	96.6	89.1	2048
ResNet-152-FC	87.6	93.3	90.7	91.2	88.3	96.7	89.4	2048

- Koch, C., Georgieva, K., Kasireddy, V., Akinci, B., Fieguth, P.: A review on computer vision based defect detection and condition assessment of concrete and asphalt civil infrastructure. *Advanced Engineering Informatics* **29**(2) (2015) 196–210
- Meijer, G.A., Beliën, J.A.M., Van Diest, P.J., Baak, J.P.A.: Image analysis in clinical pathology. *Journal of Clinical Pathology* **50**(5) (1997) 365–370
- Linder, N., Konsti, J., Turkki, R., Rahtu, E., Lundin, M., Nordling, S., Haglund, C., Ahonen, T., Pietikäinen, M., Lundin, J.: Identification of tumor epithelium and stroma in tissue microarrays using texture analysis. *Diagnostic Pathology* **7**(22) (2012) 1–11
- Nanni, L., Lumini, A., Brahnam, S.: Local binary patterns variants as texture descriptors for medical image analysis. *Artificial Intelligence in Medicine* **49**(2) (June 2010) 117–125
- Jalalian, A., Mashohor, S., Mahmud, R., Karasfi, B., Saripan, I., Ramli, A.R.: Computer-assisted diagnosis system for breast cancer in computed tomography laser mammography (ctlm). *Journal of Digital Imaging* **30**(6) (2017) 796–811
- Lowe, D.G.: Object recognition from local scale-invariant features. In: *Proceedings of Seventh IEEE International Conference on Computer Vision*, 1999. Volume 2. (1999) 1150–1157
- Serre, T., Wolf, L., Bileschi, S., Riesenhuber, M., Poggio, T.: Robust object recognition with cortex-like mechanisms. *IEEE Transactions on Pattern Analysis and*

- Machine Intelligence **29**(3) (2007) 411–426
10. Liu, H., Wu, Y., Sun, F., Guo, D.: Recent progress on tactile object recognition. *International Journal of Advanced Robotic Systems* **14**(4) (2017)
 11. Drimbarean, A., Whelan, P.: Experiments in colour texture analysis. *Pattern Recognition Letters* **22**(10) (2001) 1161–1167
 12. Mäenpää, T., Pietikäinen, M.: Classification with color and texture: jointly or separately? *Pattern Recognition* **37**(8) (2004) 1629–1640
 13. Cavina-Pratesi, C., Kentridge, R.W., Heywood, C., Milner, A.: Separate channels for processing form, texture, and color: evidence from fMRI adaptation and visual object agnosia. *Cerebral Cortex* **20**(10) (October 2010) 2319–32
 14. Palm, C.: Color texture classification by integrative co-occurrence matrices. *Pattern Recognition* **37**(5) (2004) 965–976
 15. Bianconi, F., Harvey, R., Southam, P., Fernández: Theoretical and experimental comparison of different approaches for color texture classification. *Journal of Electronic Imaging* **20**(4) (October 2011) Article number 043006.
 16. Ojala, T., Pietikäinen, M., Mäenpää, T.: Multiresolution gray-scale and rotation invariant texture classification with local binary patterns. *IEEE Transactions on Pattern Analysis and Machine Intelligence* **24**(7) (2002) 971–987
 17. Huang, D., Shan, C., Ardabilian, M., Wang, Y., Chen, L.: Local binary patterns and its application to facial image analysis: a survey. *IEEE Transactions on Systems, Man and Cybernetics Part C* **41**(6) (2017) 765–781
 18. Pietikäinen, M., Hadid, A., Zhao, G., Ahonen, T.: *Computer Vision Using Local Binary Patterns*. Volume 40 of *Computational Imaging and Vision*. Springer (2011)
 19. Brahmam, S., Jain, L., Nanni, L., Lumini, A.: Local binary patterns: new variants and applications. Volume 506 of *Studies in Computational Intelligence*. Springer (2014)
 20. Pietikäinen, M., Zhao, G.: Two decades of local binary patterns: A survey. In Bingham, E., Kaski, S., Laaksonen, J., Lampinen, J., eds.: *Advances in Independent Component Analysis and Learning Machines*. Academic Press (2015) 175–210
 21. Liu, L., Lao, S., Fieguth, P., Guo, Y., Wang, X., Pietikäinen, M.: Median robust extended local binary pattern for texture classification. *IEEE Transactions on Image Processing* **25**(3) (2016) 1368–1381
 22. Liu, L., Fieguth, P., Guo, Y., Wang, X., Pietikäinen, M.: Local binary features for texture classification: Taxonomy and experimental study. *Pattern Recognition* **62** (2017) 135–160
 23. Fernández, A., Álvarez, M.X., Bianconi, F.: Texture description through histograms of equivalent patterns. *Journal of Mathematical Imaging and Vision* **45**(1) (2013) 76–102
 24. Jin, H., Liu, Q., Lu, H., Tong, X.: Face detection using improved LBP under bayesian framework. In: *Proceedings of the 3rd International Conference on Image and Graphics*, Hong Kong, China (December 2004) 306–309
 25. Liu, L., Zhao, L., Long, Y., Kuang, G., Fieguth, P.: Extended local binary patterns for texture classification. *Image and Vision Computing* **30**(2) (2012) 86–99
 26. Bianconi, F., Fernández, A.: A unifying framework for LBP and related methods. In Brahmam, S., Jain, L.C., Nanni, L., Lumini, A., eds.: *Local binary patterns: New variants and applications*. Volume 506 of *Studies in Computational Intelligence*. Springer (2014) 17–46
 27. Charalambides, C.: *Enumerative Combinatorics. Discrete Mathematics and Its Applications*. Chapman and Hall/CRC (2002)

28. Jain, A., Healey, G.: A multiscale representation including opponent color features for texture recognition. *IEEE Transactions on Image Processing* **7**(1) (1998) 124–128
29. Mäenpää, T., Pietikäinen, M.: Texture analysis with Local Binary Patterns. In: Chen, C.H., Wang, P.S.P., eds.: *Handbook of Pattern Recognition and Computer Vision* (3rd Edition). World Scientific Publishing (2005) 197–216
30. Bianconi, F., Bello-Cerezo, R., Napoletano, P.: Improved opponent colour local binary patterns: an effective local image descriptor for colour texture classification. *Journal of Electronic Imaging* **27**(1) (2017)
31. Barnett, V.: The ordering of multivariate data. *Journal of the Royal Statistical Society. Series A (General)* **139**(3) (1976) 318–355
32. Aptoula, E., Lefèvre, S.: A comparative study on multivariate mathematical morphology. *Pattern Recognition* **40**(11) (November 2007) 2914–2929
33. Porebski, A., Vandenbroucke, N., Macaire, L.: Haralick feature extraction from LBP images for colour texture classification. In: *Proceedings of the International Workshops on Image Processing Theory, Tools and Applications (IPTA'08)*, Sousse, Tunisie (2008) 1–8
34. Barra, V.: Expanding the Local Binary Pattern to multispectral images using total orderings. In: Richard, P., Braz, J., eds.: *Proceedings of the International Conference on Computer Vision, Imaging and Computer Graphics. VISIGRAPP 2010. Volume 229 of Communications in Computer and Information Science.*, Angers, France, Springer (May 2011) 67–80
35. Ledoux, A., Richard, N., Capelle-Laizé, A.S., Fernández-Maloigue, C.: Toward a complete inclusion of the vector information in morphological computation of texture features for color images. In: *Proceedings of the 6th International Conference on Image and Signal Processing (ICISP 2014)*, Cherbourg, France (June-July 2014) 222–229
36. Ledoux, A., Losson, O., Macaire, L.: Color local binary patterns: Compact descriptors for texture classification. *Journal of Electronic Imaging* **25**(6) (2016)
37. Fernández, A., Lima, D., Bianconi, F., Smeraldi, F.: Compact colour texture descriptor based on rank transform and product ordering in the RGB color space. In: *Proceedings of the 2017 IEEE International Conference on Computer Vision Workshops (ICCVW)*. (2017)
38. Palus, H.: Representations of colour images in different colour spaces. In: *The Colour Image Processing Handbook*. Springer (1999) 67–90
39. He, K., Zhang, X., Ren, S., Sun, J.: Deep residual learning for image recognition. In: *2016 IEEE Conference on Computer Vision and Pattern Recognition*. (2016)
40. Simonyan, K., Zisserman, A.: Very deep convolutional networks for large-scale image recognition. In: *Proceedings of the 5th International Conference on Learning Representations*, San Diego, USA (May 2015)
41. Cimpoi, M., Maji, S., Kokkinos, I., Vedaldi, A.: Deep filter banks for texture recognition, description, and segmentation. *International Journal of Computer Vision* **118**(1) (2016) 65–94
42. Cusano, C., Napoletano, P., Schettini, R.: Evaluating color texture descriptors under large variations of controlled lighting conditions. *Journal of the Optical Society of America A* **33**(1) (2016) 17–30
43. Hayman, E., Caputo, B., Fritz, M., Eklundh, J.: On the significance of real-world conditions for material classification. In: *Proceedings of the 8th European Conference on Computer Vision (ECCV 2004)*. Volume 3024. (2004) 253–266

44. : The kth-tips and kth-tips2 image databases Available online at: <http://www.nada.kth.se/cvap/databases/kth-tips/download.html>. Last accessed on Jan. 11, 2017.
45. Caputo, B., Hayman, E., Mallikarjuna, P.: Class-specific material categorisation. In: Proceedings of the Tenth IEEE International Conference on Computer Vision (ICCV'05). Volume 2. (2005) 1597–1604
46. : Outex texture database Available online at <http://www.outex.oulu.fi/>. Last accessed on Jan. 12, 2017.
47. Casanova, D., Sá, J.J., Bruno, O.: Plant leaf identification using Gabor wavelets. *International Journal of Imaging Systems and Technology* **19**(3) (2009) 236–246
48. : Forestspecies database Available online at: <http://web.inf.ufpr.br/vri/image-and-videos-databases/forest-species-database>. Last accessed on Jan. 11, 2017.
49. Martins, J., Oliveira, L.S., Nigkoski, S., Sabourin, R.: A database for automatic classification of forest species. *Machine Vision and Applications* **24**(3) (2013) 567–578
50. : New [barktex] benchmark image test suite for evaluating color texture classification schemes Available online at: https://www-lisic.univ-littoral.fr/~porebski/BarkTex_image_test_suite.html. Last accessed on Jan. 12, 2017.
51. Porebski, A., Vandenbroucke, N., Macaire, L., Hamad, D.: A new benchmark image test suite for evaluating color texture classification schemes. *Multimedia Tools and Applications Journal* **70**(1) (2014) 543–556
52. : CURET: Columbia-Utrecht Reflectance and Texture Database Available online at: <http://www.cs.columbia.edu/CAVE/software/curet/index.php>. Last accessed on Jan. 25, 2017.
53. Visual Geometry Group: CURET: Columbia-Utrecht Reflectance and Texture Database Available online at: <http://www.robots.ox.ac.uk/~vgg/research/texclass/setup.html>. Last accessed on Jan. 26, 2017.
54. : Biomeditechrpe database (2016) Available online at: https://figshare.com/articles/BioMediTech_RPE_dataset/2070109. Last accessed on May 16, 2017.
55. Nanni, L., Paci, M., Santos, F.L.C., Skottman, H., Juuti-Uusitalo, K., Hyttinen, J.: Texture descriptors ensembles enable image-based classification of maturation of human stem cell-derived retinal pigmented epithelium. *Plos One* **11**(2) (2016)
56. : Breast cancer histopathological database (breackhis) (2015) Available online at <http://web.inf.ufpr.br/vri/breast-cancer-database>. Last accessed on May 16, 2017.
57. Spanhol, F., Oliveira, L.S., Petitjean, C., Heutte, L.: Breast cancer histopathological image classification using convolutional neural networks. In: International Joint Conference on Neural Networks (IJCNN 2016), Vancouver, Canada (2016)
58. : Webmicroscope. egfr colon tma stroma lbp classification (2012) Available online at: <http://fimm.webmicroscope.net/Research/Supplements/epistroma>. Last accessed on May 16, 2017.
59. : Collection of texture in colorectal cancer histology (2016) Available online at: <https://zenodo.org/record/53169#.WRsdEPmGN0w>. Last accessed on May 16, 2017.
60. Kather, J.N., Marx, A., Reyes-Aldasoro, C.C., Schad, L.R., Zöllner, F.G., Weis, C.A.: Continuous representation of tumor microvessel density and detection of angiogenic hotspots in histological whole-side images. *Oncotarget* **6**(22) (2015) 19163–19176

61. Kather, J.N., Weis, C.A., Bianconi, F., Melchers, S.M., Schad, L.R., Gaiser, T., Marx, A., Zöllner, F.G.: Multi-class texture analysis in colorectal cancer histology. *Scientific Reports* **6**(27988) (2016)
62. Bello-Cerezo, R., Bianconi, F., Cascianelli, S., Fravolini, M.L., Di Maria, F., Smeraldi, F.: Hand-designed local image descriptors vs. off-the-shelf cnn-based features for texture classification: An experimental comparison. In de Pietro, G., Gallo, L., Howlett, R., Jain, L., eds.: *Intelligent Interactive Multimedia Systems and Services (KES-IIMSS 2017)*. Volume 76 of *Smart Innovation, Systems and Technologies*. Springer, Vilamoura, Portugal (June 2017)
63. Orjuela, S., Quinones, R., Ortiz-Jaramillo, B., Rooms, F., De Keyser, R., Philips, W.: Improving textures discrimination in the local binary patterns technique by using symmetry & group theory. In: *Proceedings of the 17th International Conference on Digital Signal Processing*, Corfu, Greece (July 2011) Art. no. 6004978.